A three-dimensional synthesis study of δ 18 O in atmospheric CO 2 : 2. Simulations with the TM2 transport model

Philippe Ciais, Pieter Tans, A. Scott Denning, Roger Francey, Michael Trolier, Harro Meijer, James White, Joseph Berry, David Randall, G. James Collatz, et al.

JOURNAL OF GEOPHYSICAL RESEARCH, VOL. 102, NO. D5, PAGES 5873–5883, MARCH 20, 1997

A three-dimensional synthesis study of $\delta^{18}O$ in atmospheric CO_2 2. Simulations with the TM2 transport model

Philippe Ciais,[1] Pieter P. Tans,[2] A. Scott Denning,[3] Roger J. Francey,[4]
Michael Trolier,[25] Harro A. J. Meijer,[6] James W. C. White,[5]
Joseph A. Berry,[7] David A. Randall,[3] G. James Collatz,[8]
Piers J. Sellers,[8] Patrick Monfray,[9] and Martin Heimann[10]

Abstract. In this study, using a three-dimensional (3-D) tracer modeling approach, we simulate the $\delta^{18}O$ of atmospheric CO_2. In the atmospheric transport model TM2 we prescribe the surface fluxes of ^{18}O due to vegetation and soils, ocean exchange, fossil emissions, and biomass burning. The model simulations are first discussed for each reservoir separately, then all the reservoirs are combined to allow a comparison with the atmospheric $\delta^{18}O$ measurements made by the National Oceanic and Atmospheric Administration-University of Colorado, Scripps Institution of Oceanography-Centrum Voor Isotopen Onderzoek (United States-Netherlands) and Commonwealth Scientific and Industrial Research Organisation (Australia) air sampling programs. Insights into the latitudinal differences and into the seasonal cycle of $\delta^{18}O$ in CO_2 are gained by looking at the contribution of each source. The isotopic exchange with soils induces a large isotopic depletion over the northern hemisphere continents, which overcomes the concurrent effect of isotopic enrichment due to leaf exchange. Compared to the land biota, the ocean fluxes and the anthropogenic CO_2 source have a relatively minor influence. The shape of the latitudinal profile in $\delta^{18}O$ appears determined primarily by the respiration of the land biota, which balances photosynthetic uptake over the course of a year. Additional information on the phasing of the terrestrial carbon exchange comes from the seasonal cycle of $\delta^{18}O$ at high northern latitudes.

1. Introduction

The oxygen isotope composition of atmospheric CO_2 may yield new insight on how the terrestrial biosphere absorbs and respires CO_2. Of primary importance is the fact that CO_2 exchanges isotopically with water, according to an isotopic reaction that is catalyzed by the enzyme carbonic anhydrase. *Francey and Tans* [1987] and *Farquhar et al.* [1993] have further quantified the importance of the vegetation and soils and shown that $\delta^{18}O$ in CO_2 is linked to the gross biospheric carbon fluxes. Both the photosynthetic assimilation uptake and the total ecosystem respiration release drive the $\delta^{18}O$ in CO_2. In a companion paper [*Ciais et al.*, this issue] (hereinafter referred to as part 1) we have presented a detailed calculation of the surface fluxes that control $\delta^{18}O$ in CO_2. In the present study we prescribe these surface fluxes into a three-dimensional (3-D) model of atmospheric transport, the TM2 model [*Heimann and Keeling*, 1989; *Heimann*, 1995], in order to calculate the atmospheric $\delta^{18}O$ in CO_2 on a 7.5° horizontal grid every 3 hours.

The modeled $\delta^{18}O$ field results from exchange with five different reservoirs. Before comparing the simulated $\delta^{18}O$ with observations, we examine separately the contribution of each reservoir in order to identify the dominant mechanisms. The model results are then discussed together with atmospheric measurements at specific locations around the world. We give special attention to the latitudinal profile of $\delta^{18}O$ which is characterized by a pronounced isotopic depletion in the northern hemisphere with respect to the southern hemisphere. Also, we examine the seasonal cycle of $\delta^{18}O$ at three sites where the observational record is particularly well documented: Point Barrow (71°N), Mauna Loa (20°N), and Cape Grim (41°S).

The atmospheric observations are from flask samples collected at remote marine boundary layer sites. These measurements come from three independent air sampling networks: the National Oceanic and Atmospheric Administration-University of Colorado (NOAA-CU) network of 17 sites analyzed for ^{18}O during 1990–1994 (M. Trolier et al., An evaluation of the effects of oxygen exchange on $\delta^{18}O$ measurements from NOAA Global Air Sampling Network, submitted to *Global Biogeochemical Cycles*, 1996) (hereinafter referred to as Trolier et al., submitted manuscript, 1996), the Scripps Insti-

[1]Laboratoire de Modélisation du Climat et de l'Environnement, Commissariat à l'Energie Atomique l'Orme des Merisiers, Gif sur Yvette, France.
[2]Climate Monitoring and Diagnostic Laboratory, NOAA, Boulder, Colorado.
[3]Department of Atmospheric Sciences, Colorado State University, Fort Collins.
[4]Division of Atmospheric Research, Commonwealth Scientific and Industrial Research Organisation, Melbourne, Victoria, Australia.
[5]Institute of Arctic and Alpine Research and Department of Geological Sciences, University of Colorado, Boulder.
[6]Centrum voor Isotopen Onderzoek, University of Groningen, Groningen, Netherlands.
[7]Department of Plant Biology, Carnegie Institution of Washington, Stanford, California.
[8]NASA Goddard Space Flight Center, Greenbelt, Maryland.
[9]Centre des Faibles Radioactivités, Laboratoire de Modélisation du Climat et de l'Environnement, Gif sur Yvette, France.
[10]Max-Planck-Institut für Meteorologie, Hamburg, Germany.

Paper number 96JD02361.
0148-0227/97/96JB-02361$09.00

tution of Oceanography–Centrum voor Isotopen Onderzoek (Scripps-CIO) network of 10 sites measured between 1977 and 1992 (H. A. Meijer et al., manuscript in preparation, 1996), and the Commonwealth Scientific and Industrial Research Organisation (CSIRO) network from which we used two sites at high southern latitudes [*Francey and Tans*, 1987; *Francey et al.*, 1990, 1995]. All three experimental groups have independent sampling strategies and calibration procedures. For instance, the CSIRO group dries the air when sampling, which ensures no isotopic reaction of CO_2 and water within the flask. Nevertheless, no systematic correction was applied to the $\delta^{18}O$ data from each different group when merging the three data sets.

In this paper, sinks correspond to a negative net flux of carbon (CO_2 is removed from the atmosphere) and sources correspond to a positive net flux (CO_2 is released to the atmosphere). Isotopic ratios are expressed in per mil (‰), defined as

$$\delta^{18}O = 1000\left[\frac{(^{18}O/^{16}O)_{sample} - (^{18}O/^{16}O)_{standard}}{(^{18}O/^{16}O)_{standard}}\right]$$

For CO_2, all isotopic values are given relative to the standard isotopic ratio Vienna Pee Dee belemnite (VPDB)-CO_2 = 0.002088349077 as recommended by *Allison et al.* [1995]. For H_2O we express isotopic abundance relative to the standard Vienna SMOW (VSMOW) = 0.00200520 [*Baertchi and Macklin*, 1965]. We must subtract +41.47‰ to express VSMOW values in the VPDB-CO_2 scale. This includes a difference equivalent to −30.9‰ between VSMOW and VPDB-calcite and accounts for the ^{18}O fractionation during CO_2 evolution at 25°C with 100% phosphoric acid [*Friedman and O'Neill*, 1977] between VPDB-calcite and VPDB-CO_2.

2. Atmospheric Measurements From Three Air Sampling Programs

2.1. NOAA-CU Data

Since 1990, the Institute for Arctic and Alpine Research at the University of Colorado (CU) has been measuring the $^{13}C/^{12}C$ and $^{18}O/^{16}O$ isotope ratios of atmospheric CO_2 in flask samples of air provided by the NOAA Global Air Sampling Network. The sampling strategy and techniques (as relevant to CO_2 monitoring) have been described by *Conway et al.* [1994], while the analytical methods and calibration of the isotope data have been presented by *Trolier et al.* [1996]. The features of the sampling methodology most relevant to the $\delta^{18}O$ data are that flasks are collected in pairs as a check on sample quality and that to date, almost all the NOAA samples have been collected without drying the air prior to storage in the glass flasks. Thus, while the NOAA-CU data from high-latitude sites appear to faithfully record the $\delta^{18}O$ of atmospheric CO_2, measurements from flasks filled at more humid sampling sites are obviously contaminated, showing greatly increased differences between the two members of a pair and unrealistically rapid fluctuations. These effects have been attributed to exchange of oxygen between CO_2 and water condensed on the flasks wall [*Gemery et al.*, 1996]. Trolier et al. (submitted manuscript, 1996) have used the statistical properties of the $\delta^{18}O$ data, supplemented by comparisons of "wet" and recently available "dry" $\delta^{18}O$ data at two sites (Samoa and Cape Kumukahi), to evaluate which of the NOAA sites provide $\delta^{18}O$ data that is representative of the true atmospheric signatures.

2.2. Scripps-CIO Data

The cooperation between Scripps Institution for Oceanography and CIO (Centrum voor Isotopen Onderzoek) started in 1977. From then on, the samples from the older Scripps network for CO_2 concentration monitoring were also isotopically analyzed at CIO in Groningen, Netherlands, starting with five stations (La Jolla, Mauna Loa, Cape Kumukahi, Fanning Island, and South Pole [*Mook et al.*, 1983]), later extended over the whole Scripps monitoring network (see *Keeling et al.* [1989], who only report ^{13}C measurements). The sample handling, as well as the results of the first years of monitoring, are described by *Mook et al.* [1983]. Flask samples were taken without drying, shipped to Scripps, and analyzed for the CO_2 concentration. Then, CO_2 was extracted cryogenically and shipped to CIO, first in cork-stopped flasks, later in flame-off tubes.

At CIO the samples were measured on an (IRMS) machine, in the early years on a modified MM 903, later on a SIRA 9. All samples have been analyzed both for ^{13}C and ^{18}O. The results were corrected for the influence of N_2O [*Mook and Jongsma*, 1987]. Calibration was maintained on the basis of NBS19 carbonate, both for ^{13}C and ^{18}O. The latter scale was comaintained by using VSMOW water as reference material and checking continuously for the reproducibility of the known difference between these two primary reference materials. This has proven to be of utmost importance, since unlike for ^{13}C, the preparation route for ^{18}O involves large fractionation factors (and thus possibilities for errors). Throughout the years, several local reference materials have been used for the maintenance and checking of the calibration: carbonates, waters, and pure CO_2 standards. An extensive "history recalibration" exercise has been carried out based on multiple variable least squares techniques to reestablish the calibration of the mass spectrometers over the years, based on all the calibration measurements of primary and local standards (H. Roeloffzen, unpublished data, 1996). Final errors (random and calibration) are estimated to be ±0.025‰ for $\delta^{18}C$ and ±0.06‰ for $\delta^{18}O$, with the exception of the first several years, in which the errors were larger.

The Scripps sampling procedure did not involve drying. Although this could influence the $\delta^{18}O$ values, the overview of the isotopic data shows that this has not happened (perhaps apart from isolated clear "outliers"). The isotopic measurements on the Scripps network by CIO were terminated in 1992. From then on, isotopic measurements were carried out at Scripps itself. A full report on the Scripps-CIO data is underway.

2.3. CSIRO Data

Francey and Tans [1987] used data from five and six sites from the CSIRO global network for 1984 and 1985, respectively, and results through 1988 are presented by *Francey et al.* [1990]. Typically, 12–15 sites have been routinely sampled since the late 1980s by CSIRO. While precision is relatively high, particularly in low-latitude sites (as a result of drying all samples on collection), systematic errors are apparent in the data which are still under investigation. For this reason, only selected data from the original sites are used here. Of particular relevance is the Cape Grim in situ record, unique for the cryogenic removal of water and extraction of CO_2 on collection [*Francey et al.*, 1995]. The Cape Grim record provides a long high-precision time series permitting good definition of the small seasonality in the southern hemisphere.

3. TM2 Transport Model

We coupled the surface fluxes of $C^{18}OO$ and CO_2 with the atmospheric tracer model TM2 in order to simulate the global distribution of $\delta^{18}O$ in atmospheric CO_2. The TM model family was developed at the Max Planck Institute (Hamburg, Germany) and described by *Heimann and Keeling* [1989] for TM1 and by *Heimann* [1995] for TM2. The model grid is 7.5° by 7.5° in the horizontal, with nine vertical sigma levels and a time step of 3 hours. The horizontal mass fluxes are prescribed from the analysis of meteorological wind fields at the European Centre for Medium-Range Weather Forecasting (ECMWF) every 12 hours. The large-scale vertical mass fluxes are derived from mass continuity. Sub-grid-scale vertical transport due to both penetrative and shallow cumulus convection are calculated at each time step following the scheme of *Tiedke* [1989], together with vertical diffusion [*Louis*, 1979]. Specifically, the intensity of convective upward motion is calculated using the moisture budget at the cloud base, determined by the transported surface evaporation fluxes. The model does not have a realistic description of the stable boundary layer, which may bias the simulated surface concentrations, especially over the continents [*Denning et al.*, 1995]. For this reason, we do not consider diurnal variations in the surface fluxes.

The boundary conditions of the model are monthly fluxes of tracer averaged onto the model's grid. We verified that changing the grid of the surface fluxes conserved the total mass of tracer emitted to the atmosphere. Starting with an initial concentration field equal to zero everywhere in the atmosphere, we spun up the transport model by running the fluxes repeatedly during three model years with the atmospheric transport of 1990, then archived the simulated fourth year with the 1990 transport. For each reservoir the species CO_2 and $C^{18}OO$ are run separately, and the corresponding $\delta^{18}O$ distribution is calculated off-line after transport. Starting with tracer concentrations of zero at the beginning of the spin up, we add an arbitrary atmospheric "baseline" concentration C_{cst} to the simulated field of concentrations (see section 4.5). We thus have expressed all $\delta^{18}O$ fields in the atmosphere relative to the observed annual mean value of +0.85‰ at South Pole station.

4. Simulated $\delta^{18}O$ in CO_2

4.1. The $\delta^{18}O$ Resulting From Isotopic Exchange in Leaves

Figure 1a shows the simulated $\delta^{18}O$ of atmospheric CO_2 at the lowest model level resulting from canopy isotopic exchange. There is an Arctic minus Antarctic difference of +0.3‰, because the zonally averaged $\delta^{18}O$ value of CO_2 in leaves is greater than the atmospheric value in the northern hemisphere, except north of about 60°N (part 1, Plate 2). This confirms previous results of *Francey and Tans* [1987] and *Farquhar et al.* [1993, Figure 4] in which atmospheric mixing processes were not included. The isotopic exchange with leaves has the largest influence on atmospheric $\delta^{18}O$ over very productive source regions, especially over tropical and temperate forest ecosystems. Conversely, areas of low productivity and deserts have an almost negligible imprint on the atmospheric $\delta^{18}O$, a striking example being the fact that the broad maximum of $\delta^{18}O$ in leaf CO_2 at 30°N over the Sahara and the Middle East (Plate 2c of part 1) does not appear in the $\delta^{18}O$ distribution of Figure 1a.

There are two distinct maxima in $\delta^{18}O$ over Brazil and equatorial Africa, with values locally 1‰ above the zonal average. Similarly, there is a broad, although less pronounced maximum in $\delta^{18}O$ over Europe and North America. *Francey and Tans* [1987] suggested that low $\delta^{18}O$ values measured at Barrow (Alaska, 75°N) might be related to the isotopic exchange in leaves, but they also pointed out the need for an additional source of depleted CO_2 such as soils. In our simulation, CO_2 over Europe and eastern Siberia is more depleted in ^{18}O due to canopy exchange than Europe and western Siberia. On the other hand, Figure 1a confirms that the mechanism of leaf isotopic exchange cannot account for the observed gradient of about −1‰ between Alaska and Hawaii. This is mainly the result of lower productivity at the highest latitudes (where canopy $\delta^{18}O$ is lowest) relative to that of the temperate zone.

4.2. The $\delta^{18}O$ Resulting From Soil Exchange

Figure 1b shows the simulated atmospheric $\delta^{18}O$ surface values resulting from soil exchange. There is a −1.2‰ difference between the Arctic and the Antarctic. The latitudinal profile has a two-step shape, with one decrease between 30°S and the equator and another from 30°N to 60°N. We obtain a minimum in $\delta^{18}O$ over Siberia and over North America because CO_2 emitted by soils is isotopically depleted (Plate 1b of part 1). There are also two pronounced minima in $\delta^{18}O$ of atmospheric CO_2 over South America and Africa, both areas being characterized by a huge respiratory efflux of CO_2 that is moderately depleted in ^{18}O with respect to the atmosphere. However, it is possible that our model underestimates the $\delta^{18}O$ value of CO_2 over tropical land areas because the $\delta^{18}O$ of meteoric water that we use may be 1–2‰ lower than in the real world, based on the International Atomic Energy Agency (IAEA) measurements in precipitation in Brazil and Zimbabwe [*IAEA*, 1981; *Jouzel et al.*, 1987]. There is a sharp minimum in $\delta^{18}O$ respired by soils over equatorial Africa, in the same spot characterized by a peak in leaf $\delta^{18}O$, which is due primarily to very high productivity in this grid cell.

4.3. The $\delta^{18}O$ Resulting From the Combustion of Fossil Fuels and From Tropical Biomass

Figure 1c shows the $\delta^{18}O$ in atmospheric CO_2 caused by the burning of fossil fuels. Fossil fuel emissions deplete the northern hemisphere air in ^{18}O by 0.3‰ with respect to the southern hemisphere, because of relatively slow interhemispheric transport. The $\delta^{18}O$ decrease from south to north in Figure 1c mirrors higher concentrations of fossil CO_2 over Europe and North America. The simulated north minus south difference in fossil CO_2 is about 5 ppm. Similarly, Figure 1c shows that the $\delta^{18}O$ minima over Europe and North America correspond to maximum emissions of fossil CO_2 over industrialized regions.

Figure 1d displays the influence exerted by biomass burning emissions of CO_2 on $\delta^{18}O$ at the ground level. As expected, we model local minima in $\delta^{18}O$ of up to 0.1‰ below the zonal average over tropical regions which undergo intense biomass burning: equatorial Africa, the Amazon basin, and SE Asia. However, the isotopic depletion due to biomass burning is confined over the source regions, and the zonally averaged variation in $\delta^{18}O$ indicates only a −0.02‰ minimum around the equator. This is only a minor effect compared to fossil fuel emissions which cause a zonal mean depletion of 0.3‰ in the northern hemisphere (Figure 1d). Despite the fact that biomass burning adds 283 Tmol of CO_2 per year (3.3 GTC) to the atmospheric burden compared to 500 Tmol yr^{-1} (6 GTC) for fossil emissions, its impact on surface $\delta^{18}O$ values is diminished because strong vertical transport in the tropics prevents the

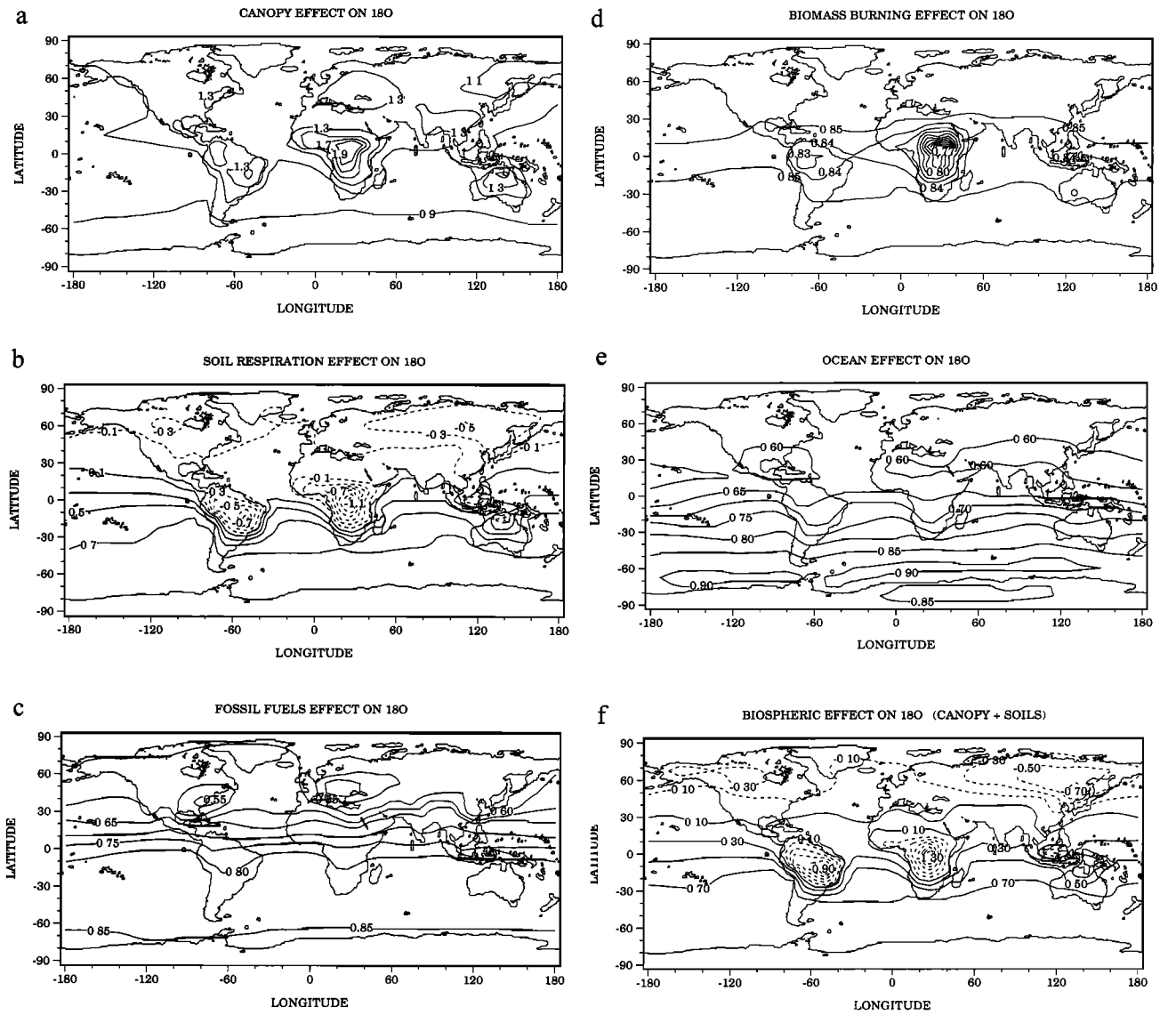

Figure 1. Annual mean $\delta^{18}O$ in CO_2 at the surface level, after transport of the surface sources by the transport model TM2. (a) The $\delta^{18}O$ resulting from leaf exchange. (b) The $\delta^{18}O$ resulting from soil respiration. (c) The $\delta^{18}O$ resulting from fossil fuel emissions. (d) The $\delta^{18}O$ resulting from air-sea exchange. (e) The $\delta^{18}O$ resulting from biomass burning emissions. (f) "Biospheric" $\delta^{18}O$, combination of leaf exchange and soil respiration. All fields are plotted relative to the observed South Pole station annual mean value of +0.85‰.

CO_2 emitted by fires to build up at the surface level. In other words, the tropical biomass burning source is diluted in the vertical, whereas the fossil source is more confined near the surface.

4.4. The $\delta^{18}O$ Resulting From Ocean Isotopic Exchange

Figure 1e shows the simulated $\delta^{18}O$ in atmospheric CO_2 at the surface as resulting from ocean exchange. There is a permanent negative difference in $\delta^{18}O$ of −0.3‰ between the north and the south, the largest decrease taking place between approximately 40°S and 10°N. This latitudinal difference can be compared with Plate 3b of part 1, representing $\delta^{18}O$ of CO_2 dissolved in the ocean. Although high-latitude oceans in both hemispheres are enriched in ^{18}O to similar magnitudes, there is a much greater ocean area in the south, which likely causes the decrease in $\delta^{18}O$ from south to north apparent in Figure 1e. Additionally, the air-sea gas exchange in the southern ocean is more vigorous than over the northern oceans [*Erickson*, 1993].

Locally, at around 60°S, stronger winds enhance the transfer of enriched CO_2 dissolved in surface waters to the atmosphere, yielding maximum values in $\delta^{18}O$ which decrease farther to the south, over Antarctica. There is little longitudinal variation in $\delta^{18}O$ resulting from ocean exchange. However, Figure 1e indicates two "tongues" of northern hemisphere air depleted in ^{18}O over South America and Africa, the passage of northern hemisphere air across the equator being facilitated over the tropical continents, as previously noticed in ^{85}Kr simulations with the TM1 model by *Heimann and Keeling* [1989] (the TM2 model is close to TM1 for ^{85}Kr).

4.5. Combined $\delta^{18}O$ Fields

The atmospheric "total" $\delta^{18}O$, corresponding to exchange with all reservoirs, δ_a, is obtained from the combination of the concentration fields due to each separate reservoir. In every

grid box of the atmospheric model we calculate the total $\delta^{18}O$ using

$$\delta_a = \left[\frac{{}^{18}C_o + {}^{18}C_L + {}^{18}C_s + {}^{18}C_{fos} + {}^{18}C_{bur} + {}^{18}C_{cst}}{C_o + C_L + C_s + C_{fos} + C_{bur} + C_{cst}} \Big/ R_{PDB} - 1 \right] 1000$$

where

$C_o({}^{18}C_o)$ CO_2 ($C^{18}OO$) mixing ratio resulting from exchange with ocean;

$C_L({}^{18}C_L)$ CO_2 ($C^{18}OO$) mixing ratio resulting from exchange with leaves;

$C_s({}^{18}C_s)$ CO_2 ($C^{18}OO$) mixing ratio resulting from exchange with soils;

$C_{fos}({}^{18}C_{fos})$ CO_2 ($C^{18}OO$) mixing ratio resulting from fossil fuel emissions;

$C_{bur}({}^{18}C_{bur})$ CO_2 ($C^{18}OO$) mixing ratio resulting from biomass burning;

C_{cst} assumed mean atmospheric CO_2 mixing ratio, constant everywhere, over which are superimposed the anomalies in CO_2 due to exchange with the surface sources (C_{cst} = 355 ppm);

${}^{18}C_{cst}$ assumed mean atmospheric $C^{18}OO$ mixing ratio, constant everywhere, over which are superimposed the anomalies in $C^{18}OO$ due to exchange with the surface sources (${}^{18}C_{cst}$ corresponds to the mean South Pole station value of $\delta^{18}O$ = 0.85‰ and thus is equal to C_{cst} [1 + (0.85/1000)] R_{PDB}).

4.6. Combination of Vegetation and Soils (Biospheric $\delta^{18}O$)

Figure 1f shows the $\delta^{18}O$ resulting from soil and leaf exchange combined, all other sources being set to zero in the equation given in section 4.5. While leaves and soils separately generate north minus south differences in atmospheric $\delta^{18}O$ of similar amplitude but opposite in sign (Figures 1a and 1b), the superposition of both yields a net negative north minus south latitudinal difference of −0.9‰. The biospheric $\delta^{18}O$ at the surface level has two main regional minima, corresponding to an isotopic depletion of the atmospheric reservoir: one over the eastern part of Siberia and another over the Amazon. Over these areas the exchange with the land biota determines $\delta^{18}O$ values that are typically 0.6‰ below the zonal average.

Despite the fact that the annual mean uptake of CO_2 by canopy photosynthesis (A) is locally equal to the release of CO_2 by respiration ($\Re$), the soil source has a larger influence on the atmospheric $\delta^{18}O$ because CO_2 in soils bears a larger isotopic disequilibrium with respect to the atmosphere than CO_2 in leaves (compare Plates 1b and 2c of part 1). Another factor which contributes an additional asymmetry between the vegetation and the soils is the fact that the atmospheric circulation tends to accumulate some CO_2 issued from soil respiration over continental Asia due to seasonal differences in the vertical and southward transport intensity [*Keeling et al.*, 1989; *Denning et al.*, 1995]. Since CO_2 from soils has a lower $\delta^{18}O$ value than CO_2 from leaves, this pattern of the northern hemisphere circulation decreases the $\delta^{18}O$ in the atmosphere over Siberia due to the accumulation of respired CO_2 near the surface over that region (Figure 1f).

4.7. Combination of All Reservoirs

The $\delta^{18}O$ in atmospheric CO_2 in the lowest model layer resulting from exchange with all reservoirs is shown in Figure 2. Comparison of Figure 2 with Figure 1c shows that the total $\delta^{18}O$ is dominated by terrestrial processes. There is a decrease in $\delta^{18}O$ from south to north of 1.5‰, mostly contributed by soils and to a lesser extent by fossil CO_2. There are also important longitudinal variations characterized by large negative anomalies in $\delta^{18}O$ over the continents, which are due to soil respired CO_2. In the latitude band around 65°N, we simulate an east-west difference of −0.6‰ in $\delta^{18}O$ between Siberia and the North Atlantic. Around the equator, we obtain two pronounced $\delta^{18}O$ minima both over the Amazon basin and over Equatorial Africa, with an additional decrease in atmospheric $\delta^{18}O$ over SE Asia. Such large longitudinal differences in the simulated $\delta^{18}O$ fields have no equivalent in the CO_2 distribution because the isotopic exchange with the biosphere is more vigorous than for CO_2, due to the isotopic disequilibrium fluxes (part 1).

5. Comparison With $\delta^{18}O$ Measurements

5.1. North Minus South Differences in $\delta^{18}O$

Figure 3 compares the zonally averaged simulated $\delta^{18}O$ field with the NOAA-CU, Scripps-CIO, and CSIRO observations, all zonal profiles being referenced relative to the value of +0.85‰ at the South Pole (the observed average $\delta^{18}O$ measured by CSIRO at the station in 1990). We simulate a decrease in total $\delta^{18}O$ from south to north of −1.5‰, comparable in magnitude to the observed pattern. There are two steps on the simulated average $\delta^{18}O$: a first drop of −1‰ between 40°S and the equator, and a smoother decrease of −0.5‰ between 0 and 60°N. North of 60°N, $\delta^{18}O$ slightly increases by 0.1‰.

The atmospheric measurements also suggest a two-step decrease from south to north, although all tropical sites are measured without drying the air, which gives us less confidence in the measured $\delta^{18}O$. Yet the model fails to predict high enough $\delta^{18}O$ values between 0 and 40°N. As an example, at Fanning Island (3°N, Scripps-CIO site LIN in Figure 3), Mauna Loa (19.5°N, NOAA-CU and Scripps-CIO site MLO in Figure 3), and La Jolla (32.9°N Scripps-CIO site LJO in Figure 3), our calculations underestimate $\delta^{18}O$ by roughly 0.5‰. A second discrepancy between model and observations exists at high northern latitudes, where the simulated $\delta^{18}O$ values are 0.2‰ above the observations. The data indicate a marked drop in $\delta^{18}O$ of about −1‰ between La Jolla and Barrow, whereas we model a decrease of less than −0.5‰. In the southern tropics we slightly underestimate the $\delta^{18}O$ compared to the measurements on the NOAA-CU ship cruises (sites S35 to S25 on Figure 3), but this needs to be confirmed by measurements made on dry air samples.

Figure 3 indicates that the $\delta^{18}O$ obtained in the model at Fanning Island (3°N, Scripps-CIO site denoted LIN in Figure 3) is 0.3‰ above the calculated zonal mean value at this latitude. This model feature is due to minima in $\delta^{18}O$ over equatorial Africa and Brazil (Figure 2) which make the zonal mean $\delta^{18}O$ lower than the value calculated at a remote maritime site. This raises a cautionary flag about the zonal representativeness of the existing marine boundary layer stations where $\delta^{18}O$ is routinely measured. Similarly, strong $\delta^{18}O$ differences between ocean and continent at high northern latitudes may explain why $\delta^{18}O$ is higher at Iceland (20°W; 63°N denoted ICE in Figure 3) than at Cold Bay (163°W; 55°N denoted CBA) and at Barrow (156°W; 71°N denoted BRW),

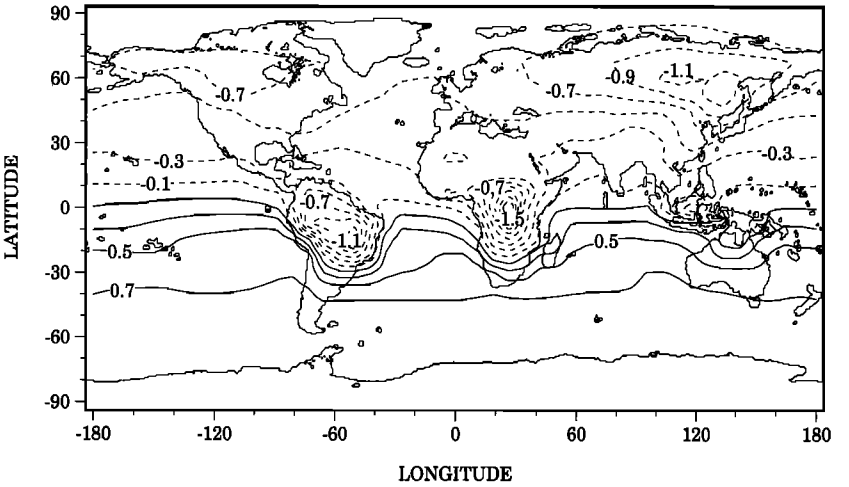

Figure 2. Annual mean $\delta^{18}O$ in CO_2 at the surface level resulting of terrestrial fluxes, air-sea exchange, and anthropogenic CO_2 emissions (combination of all reservoirs).

both in the model and on the NOAA-CU and Scripps-CIO observations (Figure 3).

A better understanding of the discrepancies between this standard experiment and the $\delta^{18}O$ measured at the stations will require a full study of the sensitivity of our model to its prescribed parameters. One can distinguish two types of parameters, related on one hand to the isotopic hydrology (i.e., $\delta^{18}O$ of H_2O in leaves and soils) and on the other hand to the biospheric carbon fluxes (i.e., assimilation A and total respiration $\Re$). A detailed study to separate these two components of the ^{18}O cycle of CO_2 will be presented elsewhere.

5.2. Point Barrow, Alaska, 71°N (NOAA-CU)

Figure 4a shows the simulated monthly means of CO_2 and $\delta^{18}O$ at Barrow together with the NOAA-CU measurements. Both model results and observations are detrended. The $\delta^{18}O$ annual cycle simulated for 1990 is repeated identically two times and plotted against the observations during the interval

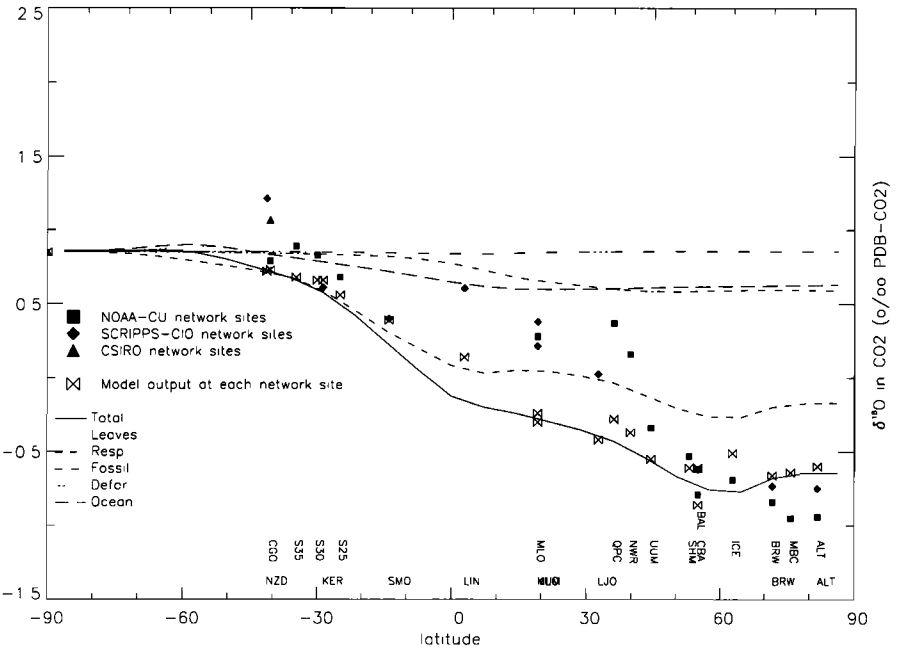

Figure 3. Zonally averaged latitudinal profile of $\delta^{18}O$ in CO_2 at the surface. The different curves separate the exchange with leaves, soils, ocean, fossil emissions, and biomass burning. Note that the $\delta^{18}O$ profiles pertaining to each reservoir are not additive but rather combine linearly to yield the resultant $\delta^{18}O$ curve in solid line. Solid symbols correspond to the $\delta^{18}O$ simulated at the precise location of the air sampling sites and are the average of atmospheric data measured on flasks samples by NOAA-CU (squares), Scripps-CIO (diamonds), and by CSIRO (triangles). At least 2 years of data have been averaged in the atmospheric measurements shown here.

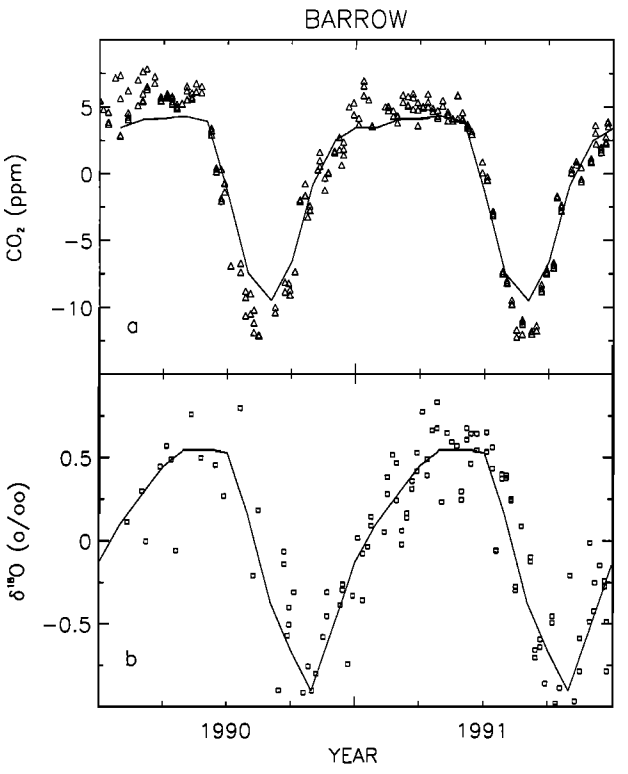

Figure 4a. Atmospheric CO_2 and $\delta^{18}O$ simulated at Point Barrow, Alaska (71°N), compared with the NOAA-CU flask measurements. Both the data and the model output have been detrended.

1990–1991. The model matches well the observed seasonality of the CO_2 annual cycle, but it underestimates the peak-to-peak amplitude by about 3 ppm. The simulated $\delta^{18}O$ seasonal cycle is in very good agreement with the seasonality of the observations. The model reproduces well the observed position of the minimum in $\delta^{18}O$ during October–November. The simulated peak-to-peak amplitude of $\delta^{18}O$ at Barrow is 1.44‰ compared to a range of 1.2–1.5‰ in the NOAA-CU measurements.

Figure 4b separates $\delta^{18}O$ at Barrow into its different components. The seasonality in $\delta^{18}O$ due to fossil emissions and ocean exchange is negligible. The isotopic exchange with soils contributes roughly ¾ of the total amplitude and largely determines the phase of the simulated total $\delta^{18}O$. Specifically, Figure 4b indicates that the October–November minimum in total $\delta^{18}O$ at Barrow is due to soil exchange, resulting from the seasonal variation of $\delta^{18}O$ in soil CO_2 multiplied by the $\mathfrak{R}$ flux (see part 1, equation (3)). In order to confirm this hypothesis we calculated the average $\delta^{18}O$ of soil CO_2 over the Siberian region (the region which exerts the largest influence on the concentrations at Barrow) and verified that this variable reaches a minimum in October–November. At this time of the year the $\mathfrak{R}$ flux is still large enough for such a minimum in $\delta^{18}O$ of soil CO_2 to have a significant imprint on the atmospheric $\delta^{18}O$ at Barrow ($\mathfrak{R}$ in fall over Siberia is ~30% of its maximum level in August).

Figure 4b also suggests that canopy exchange has a smaller influence than soils on the seasonality of $\delta^{18}O$ at Barrow, contributing a slight increase in $\delta^{18}O$ from April to June and then virtually no change between August and December. Such

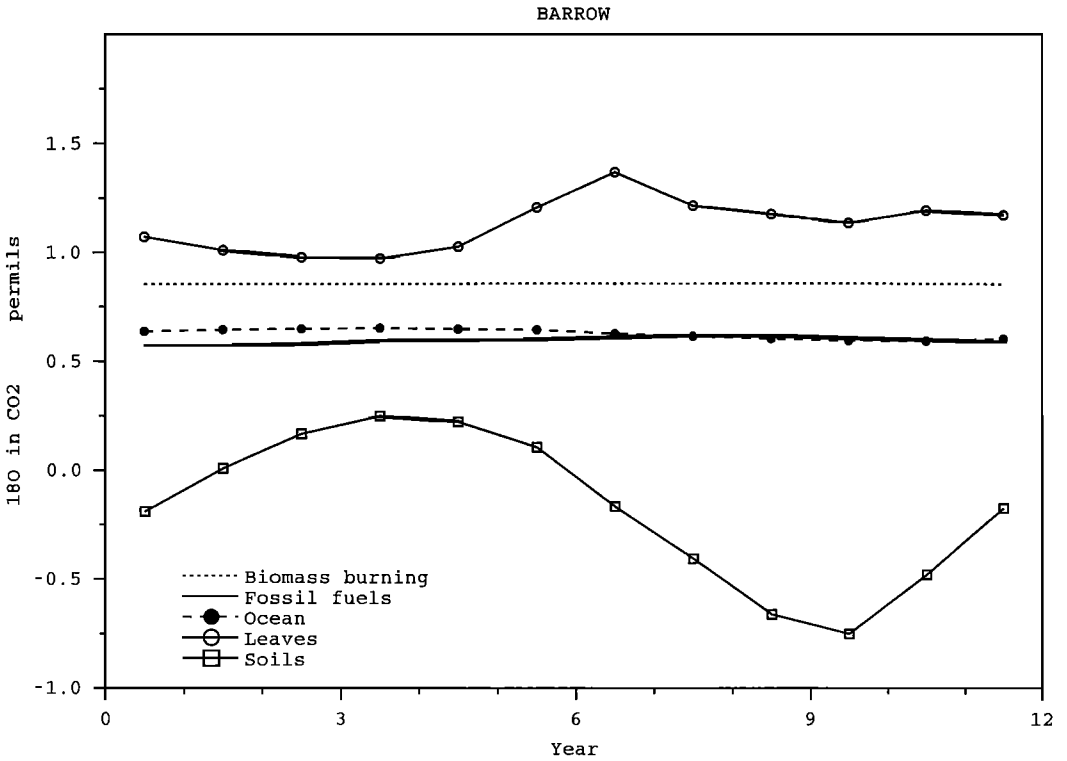

Figure 4b. Modeled $\delta^{18}O$ decomposed into components resulting from exchange with each reservoir separates. Triangles, leaves; squares, soils; short dashed line, ocean; long dashed line, fossil emissions; solid line, biomass burning.

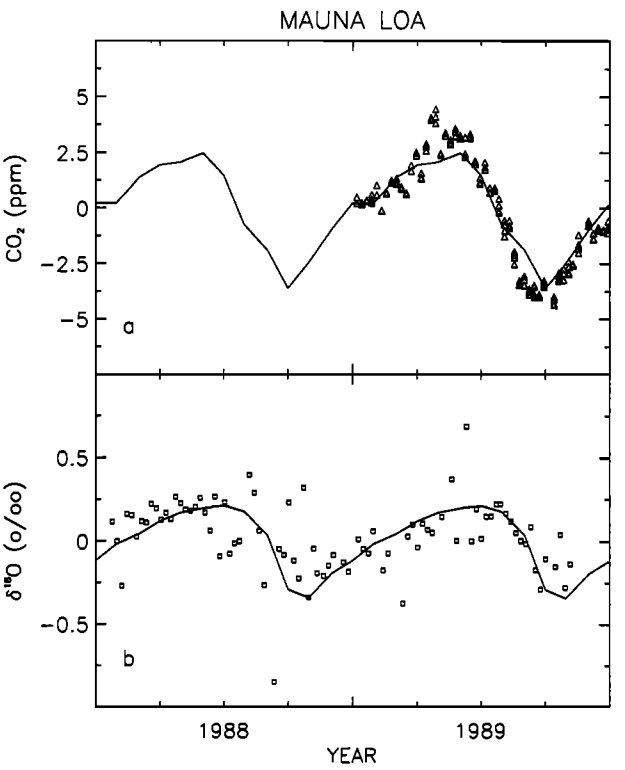

Figure 5a. Atmospheric CO_2 and $\delta^{18}O$ simulated at Mauna Loa, Hawaii (3400 m, 19°N), compared with the Scripps-CIO flask measurements. Both the data and the model output have been detrended.

a weak influence of the leaf isotopic exchange on the seasonality of total $\delta^{18}O$ at Barrow, especially during the growing season is surprising. It can be explained by equation (7) of part 1, in which the canopy isotopic disequilibrium flux is treated as the product of the retrodiffused flux of CO_2 and $\delta^{18}O$ in leaf CO_2. The simulated monthly mean $\delta^{18}O$ of leaf CO_2 over Siberia is nearly constant during the summer and the fall. As the $\delta^{18}O$ in leaf CO_2 is a decreasing function of temperature and an increasing function of $\delta^{18}O$ in leaf water (part 1, equation (12)), higher temperatures in summer compensate for higher $\delta^{18}O$ in leaf CO_2. In spring, however, relatively cold temperatures cause $\delta^{18}O$ to rise in leaf CO_2, contributing the increase in May–June in the vegetation $\delta^{18}O$ exchange at Barrow on Figure 4b.

5.3. Mauna Loa, Hawaii, 19°N (Scripps-CIO)

Figure 5a shows the observed and simulated seasonal cycle of CO_2 and $\delta^{18}O$ at Mauna Loa, a station located at sigma level 3 in the TM2 model. Both model results and observations are detrended. We have repeated two times the $\delta^{18}O$ annual cycle simulated for 1990 and plotted it against observations during the 1988–1989 period. Our model underestimates the peak-to-peak amplitude in CO_2 by 2 ppm at Mauna Loa, although the phase is approximately correct. The simulated $\delta^{18}O$ peak-to-peak amplitude is also too small in our model (0.4‰) compared to the Scripps-CIO measurements (0.6‰). On the other hand, the phase of the $\delta^{18}O$ model curve is realistic and indicates that $\delta^{18}O$ at Mauna Loa is maximum in June–July, then decreases sharply during August to reach a minimum in September–October. The lag of the $\delta^{18}O$ versus CO_2 minimum at

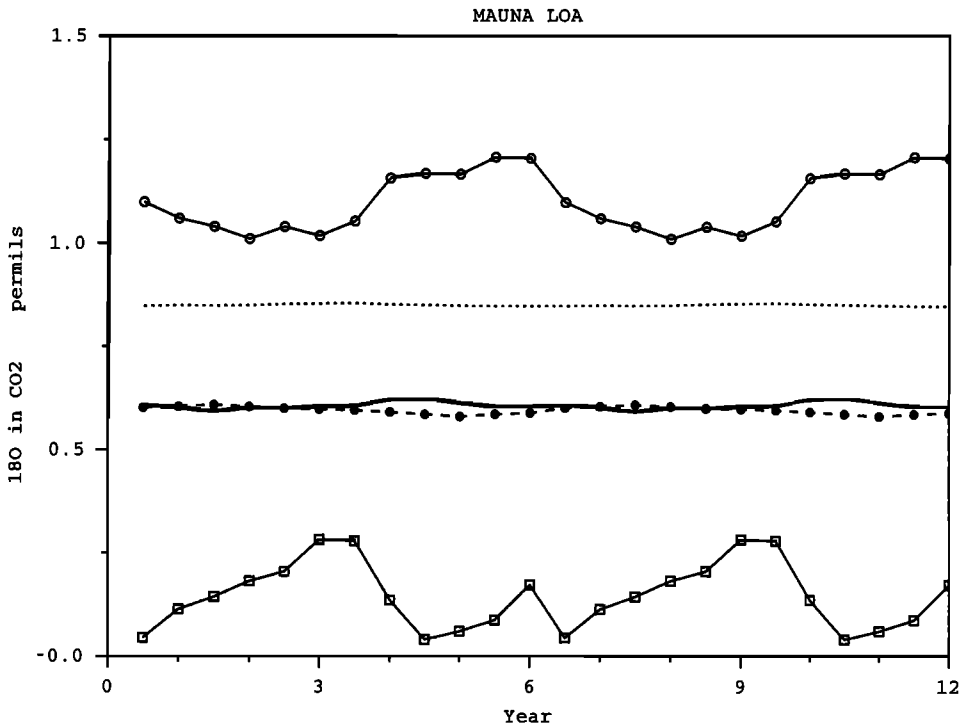

Figure 5b. Modeled atmospheric $\delta^{18}O$ decomposed into components resulting from exchange with each reservoir separates. Triangles, leaves; squares, soils; short dashed line, ocean; long dashed line, fossil emissions; solid line, biomass burning.

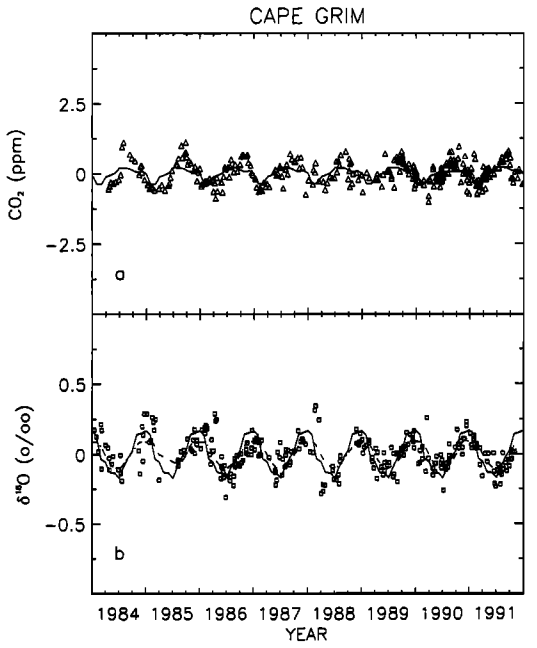

Figure 6a. Atmospheric CO_2 and $\delta^{18}O$ simulated at Cape Grim, Tasmania (41°S). The $\delta^{18}O$ is from the CSIRO flasks and CO_2 from the NOAA flasks. Both the data and the model output have been detrended. The dashed line in the $\delta^{18}O$ plot is a periodic fit to the data composed of four harmonics.

Mauna Loa is less than a month, compared to 2 months at Barrow.

Figure 5b separates $\delta^{18}O$ at Mauna Loa into its different components. As is the case at Barrow, the isotopic exchange with soils is found to be the dominant component of the seasonal cycle. However, canopy exchange contributes proportionally more to the seasonality of total $\delta^{18}O$ at Mauna Loa than at Point Barrow (⅓ for leaves versus ⅔ for soils). Leaf isotopic exchange causes an increase in $\delta^{18}O$ at Mauna Loa by 0.2‰ during July–August, then a plateau between August and December followed by a decrease of 0.2‰ in January–February. The ocean and fossil fuel components both induce a weak seasonality in $\delta^{18}O$, which is due primarily to the seasonal variation in atmospheric transport.

5.4. Cape Grim, Tasmania, 41°S (CSIRO)

Figure 6a compares the modeled CO_2 and $\delta^{18}O$ at Cape Grim to the measurements made on air samples collected and analyzed at CSIRO between 1982 and 1992 for $\delta^{18}O$ (the CO_2 data are from NOAA flasks). Since our model does not include any year-to-year variability in the $\delta^{18}O$ sources, we have repeated the $\delta^{18}O$ annual cycle simulated for 1990 over the interval 1984–1992. The detrended observations have been fitted with a periodic function containing four harmonics. The model correctly simulates the phase of $\delta^{18}O$ at Cape Grim, with a maximum in December (summer) and minimum in June (winter). The simulated peak-to-peak amplitude (0.35‰) is

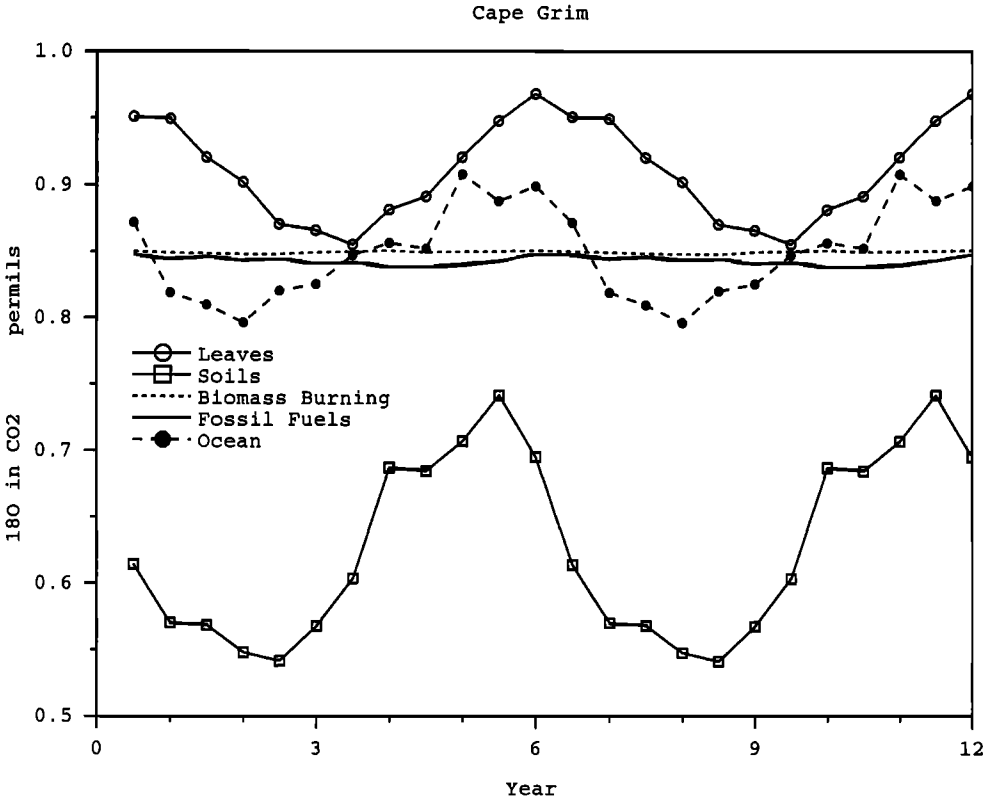

Figure 6b. Model atmospheric $\delta^{18}O$ decomposed into components resulting from exchange with each reservoir separates. Triangles, leaves; squares, soils; short dashed line, ocean; long dashed line, fossil emissions; solid line, biomass burning.

1.6 times larger than the average observed peak-to-peak amplitude during 1982–1992 (0.21‰). Note that we do not apply any selection criteria on the model output to account for the fact that flasks are sampled only when the air comes from a "clean air" sector. According to *Ramonet and Monfray* [1996], selecting the model output for the clean air sector at Cape Grim substantially damps the seasonal cycle of CO_2 at Cape Grim by removing large synoptic anomalies associated to non-background conditions.

Figure 6b separates $\delta^{18}O$ into its different components. The ocean contributes 40% of the total $\delta^{18}O$ amplitude at Cape Grim, and the biosphere (vegetation plus soils) contributes 60%. Fossil CO_2 has a negligible impact on the seasonal cycle of $\delta^{18}O$. The seasonal cycle due to ocean isotopic exchange is minimum in May and maximum in October–December. It is not obviously correlated with the seasonal cycle of SST in the southern ocean since during the Austral summer, warmer SSTs decrease the $\delta^{18}O$ of CO_2 in seawater (part 1, equation (16)). The exchange with the land biota causes $\delta^{18}O$ at Cape Grim to be higher in summer and a lower in winter. *Ramonet* [1994] calculates that at 40°S the effects of biospheric exchange in the northern and southern hemispheres are roughly in phase after a lag of about 6 months due to atmospheric transport.

The $\delta^{18}O$ 10-year record of Cape Grim from *Francey et al.* [1995, Figure 4] indicates that significant year-to-year variations occur whose origin is not clearly known. It is likely that interannual variations in the sources of ^{18}O may have caused the large positive anomalies observed in 1983–1984, 1987–1988, and 1990–1991. Strong $\delta^{18}O$ positive anomalies appear to occur soon after an El Niño event. Considering that El Niño episodes are associated with anomalously high SSTs over the eastern Pacific, it is possible that the ocean cooling associated with a return to normal conditions after an El Niño year may cause a small increase in $\delta^{18}O$. However, the biosphere on land is also likely to have contributed to the interannual variations in the $\delta^{18}O$ of atmospheric CO_2, linked to changes in photosynthesis, respiration [*Keeling et al.*, 1995] and in global hydrology.

6. Conclusions

We have calculated the atmospheric distribution of the $\delta^{18}O$ in atmospheric CO_2 resulting from exchange with leaves, soils, ocean, and anthropogenic emissions. The monthly exchange fluxes derived in part 1 have been run in the 3-D atmospheric transport model TM2 in order to simulate the field of $\delta^{18}O$ in atmospheric CO_2 on a 7.5° horizontal grid at nine vertical levels. The simulated $\delta^{18}O$ values have been compared to recent measurements made by three independent air sampling programs at NOAA-CU, Scripps-CIO, and CSIRO.

As anticipated by the previous study of *Farquhar et al.* [1993], which did not explicitly include the atmospheric transport, we found that the terrestrial biosphere dominates the spatial and seasonal variations of atmospheric $\delta^{18}O$ values, whereas the oceanic exchange plays a relatively minor role. Our main result is that vigorous ^{18}O exchange with soils is primarily responsible for the persistent depletion in $\delta^{18}O$ over the high latitudes of the northern hemisphere. Leaf isotopic exchange opposes this effect by causing an isotopic enrichment in the northern hemisphere. In the tropics we predict a depletion in ^{18}O of CO_2 over regions covered by tropical evergreen forests, an interesting result that would need to be tested against data from continental sites, for example, by airborne measurements. Overall, the annual ecosystem respiration strongly modulates the shape of the latitudinal profile in $\delta^{18}O$. Since the annual mean respiration roughly equals the uptake by photosynthesis, we believe that $\delta^{18}O$ does yield independent information on the large-scale geographical distribution of the gross terrestrial carbon fluxes.

We have also examined the seasonality of $\delta^{18}O$ at a few sites and find that the $\delta^{18}O$ seasonal cycle is controlled by the temporal variation in respiration and photosynthesis. In the northern hemisphere a detailed study of the seasonal cycle at Point Barrow and Mauna Loa underscores the key influence of soil respiration in explaining the observed phase lag of $\delta^{18}O$ versus CO_2. Finally, at Cape Grim in the southern hemisphere, the ocean appears to contribute roughly one third of the observed seasonal cycle. The long time series of Cape Grim suggests that large interannual variations are superimposed to the average seasonal cycle.

At this stage the $\delta^{18}O$ of CO_2 can not yet be used quantitatively to infer the terrestrial fluxes of CO_2 because we did not examine the sensitivity of our calculations to the prescribed parameters of the model. Of particular importance are the factors that control $\delta^{18}O$ of water in the soil and in chloroplasts, mainly the isotopic composition of water vapor and the relative humidity within the canopy. Another important improvement would be to design a global model of the isotopic composition of CO_2 which includes both a coupling of photosynthesis with climate as already done in SiB2 and a parameterization of the isotopic composition of water. In addition, the atmospheric transport should be entirely consistent with the calculated surface fluxes.

Acknowledgments. We thank J. M. Hirtzmann and S. Fauquet for carrying out a preliminary modeling study. We are especially grateful to G. D. Farquhar, C. A. M. Brenninkmeijer, and K. Rozanski for helpful discussions on this work. P. Gemery, D. Young, C. Brock, D. Bryant, D. Decker, and S. Webb made the isotopic analysis of the NOAA/CU flasks. T. Conway and N. Zhang are responsible for the analyses of CO_2, and L. Waterman is responsible for the logistics of the NOAA/CMDL network. We thank the Cape Grim Baseline Air Pollution Station, the Australian Antarctic Division, and the CSIRO's GASLAB for the Cape Grim and south pole data. Partial support was provided by the Ocean and Atmosphere Carbon Exchange Study and the Atmospheric Chemistry projects of the Climate and Global Change Program of NOAA and by the Atmospheric Research and Exposure Assessment Laboratory of the EPA. The French Programme National d'Etude de la Dynamique du Climat and Commissariat à l'Energie Atomique also contributed to funding. Support is also provided by the EC program ESCOBA.

References

Allison, C. E., R. J. Francey, and H. A. Meijer, Recommendations for the reporting of stable isotope measurements of carbon and oxygen in CO_2 gas, in *References and Intercomparison Materials for Stable Isotopes of Light Elements, Proceedings of a Consultants Meeting Held in Vienna, 1–3 December 1993, IAEA-TECDOC-825*, pp. 155–162, Int. At. Energy Agency, Vienna, 1995.

Baertchi, I. H., and W. C. Macklin, Absolute ^{18}O content of standard mean ocean water, *Earth Planet. Sci. Lett.*, *31*, 341–344, 1965.

Ciais, P., et al., A three-dimensional synthesis study of $\delta^{18}O$ in atmospheric CO_2, 1, Surface fluxes, *J. Geophys. Res.*, this issue.

Conway, T. J., P. P. Tans, L. S. Waterman, K. W. Thoning, D. R. Kitzis, K. A. Masarie, and N. Zhang, Evidence for interannual variability of the carbon cycle from the National Oceanic and Atmospheric Administration/Climate Monitoring and Diagnostic Laboratory Global Air Sampling Network, *J. Geophys. Res.*, *99*, 22,831–22,855, 1994.

Denning, A. S., I. Y. Fung, and D. A. Randall, Latitudinal gradient of atmospheric CO_2 due to seasonal exchange with biota, *Nature*, *376*, 240–243, 1995.

Erickson, D. J., III., A stability dependent theory for air-sea exchange, *J. Geophys. Res.*, *98*, 8471–8488, 1993.

Farquhar, G. D., J. Lloyd, J. A. Taylor, L. B. Flanagan, J. P. Syvertsen, K. T. Hubick, S. C. Wong, and R. Ehleringer, Vegetation effects on the isotope composition of oxygen in atmospheric CO_2, *Nature*, *363*, 439–443, 1993.

Francey, R. J., and P. P. Tans, Latitudinal variation in oxygen-18 of atmospheric CO_2, *Nature*, 495–497, 1987.

Francey, R. J., F. J. Robbins, C. E. Allison, and N. G. Richards, The CSIRO global survey of CO_2 stable isotopes, in *Baseline Atmospheric Research Program (Australia) 1988*, edited by S. R. Wilson and G. P. Ayers, pp. 20–27, Common. Sci. Ind. Res. Organ. Div. Atmos. Res., Melbourne, Victoria, Australia, 1990.

Francey, R. J., C. E. Allison, and E. D. Welch, The 11-year high precision in situ CO_2 stable isotope record from Cape Grim, 1982–1992, in *Baseline Atmospheric Research Program (1992)*, edited by C. Dick and P. J. Fraser, pp. 16–25, Commw. Sci. Ind. Res. Organ. Div. Atmos. Res., Melbourne, Victoria, Australia, 1995.

Friedman, I., and J. R. O'Neill, Compilation of stable isotope fractionation factors of geochemical interest, *Pap. 440-KK*, U.S. Geol. Surv., Reston, Va., 1977.

Gemery, P. A., M. Trolier, and J. W. C. White, Oxygen isotope exchange between carbon dioxide and water following atmospheric sampling using glass flasks, *J. Geophys. Res.*, *101*, 14,415–14,420, 1996.

Heimann, M., *The Global Atmospheric Tracer Model TM2*, Dsch. Klimarechenzentrum Modellbetreuungsgruppe, Hamburg, Germany, 1995.

Heimann, M., and C. D. Keeling, A three dimensional model of atmospheric CO_2 transport based on observed winds, 2, Model description and simulated tracer experiments, in *Aspects of Climate Variability in the Pacific and Western Americas*, *Geophys. Monogr. Ser.*, vol. 55, edited by D. H. Peterson, pp. 237–275, AGU, Washington, D. C., 1989.

International Atomic Energy Agency (IAEA), Statistical treatment of environmental isotope data in precipitation, *Tech. Rep. Ser. I.A.E.A.*, *206*, 1–256, 1981.

Jouzel, J., G. L. Russell, R. J. Suozzo, R. D. Koster, J. W. C. White, and W. S. Broecker, Simulations of the HDO and H_2 ^{18}O atmospheric cycles using the NASA/GISS general circulation model: The seasonal cycle for present-day conditions, *J. Geophys. Res.*, *92*, 14,739–14,760, 1987.

Keeling, C. D., Piper, S. C., and M. Heimann, A three-dimensional model of atmospheric CO_2 transport based on observed winds, 4, Mean annual gradients and interannual variations, in *Aspects of Climate Variability in the Pacific and Western Americas*, *Geophys. Monogr. Ser.*, vol. 55, edited by D. H. Peterson, pp. 305–363, AGU, Washington, D. C., 1989.

Keeling, C. D., T. P. Whorf, M. Wahlen, and J. Van der Plicht, Interannual extremes in the rate of rise of atmospheric carbon dioxide since 1980, *Nature*, *375*, 666–670, 1995.

Louis, J. F., A parametric model of vertical eddy fluxes in the atmosphere, *Boundary Layer Meteorol.*, *17*, 187–202, 1979.

Mook, W. G., and J. Jongsma, Measurement of the N_2O correction for $^{13}C/^{12}C$ ratios of atmospheric CO_2 by removal of N_2O, *Tellus*, *39*, 96–99, 1987.

Mook, W. G., M. Koopmans, A. F. Carter, and C. D. Keeling, Seasonal, latitudinal, and secular variations in the abundance and isotopic ratios of atmospheric carbon dioxide, 1, Results from land stations, *J. Geophys. Res.*, *88*, 10,915–10,933, 1983.

Ramonet, M., Variabilité du CO_2 atmosphérique en régions australes: Comparaison modèle et mesures, Ph.D. thesis, Univ. Paris XI, Paris, 1994.

Ramonet, M., and P. Monfray, CO_2 baseline concept in 3-D atmospheric transport models, *Tellus*, *Ser. B*, *48*, 502–520, 1996.

Tiedke, M., A comprehensive mass flux scheme for cumulus parametrization in large-scale models, *Mon. Weather Rev.*, *117*, 1779–1800, 1989.

Trolier, M., J. W. C. White, P. P. Tans, K. A. Masarie, and P. A. Gemery, Monitoring the isotopic composition of atmospheric CO_2: Measurements from the NOAA global air sampling network, *J. Geophys. Res.*, *101*, 25,897–25,916, 1996.

J. A. Berry, Department of Plant Biology, Carnegie Institution of Washington, 290 Panama Street, Stanford, CA 94305. (e-mail: joeberry@biosphere.stanford.edu)

P. Ciais, LMCE, CEA l'Orme des Merisiers, Commissariat à l'Energie Atomique, Bâtiment 709, Saclay 91191 Gif sur Yvette, France. (e-mail: ciais@obelix.saclay.cea.fr)

G. J. Collatz and P. J. Sellers, NASA Goddard Space Flight Center, MC 923, Biosphere Sciences Branch, Greenbelt, MD 20771.

A. S. Denning and D. A. Randall, Department of Atmospheric Sciences, Colorado State University, Fort Collins, CO 80523-1370. (e-mail: scott@abyss.atmos.colostate.edu)

R. J. Francey, Division of Atmospheric Research, CSIRO, PMB Aspendale, Melbourne, Victoria 3195, Australia.

M. Heimann, Max-Planck Institut für Meteorologie, Bundestrasse 55, D-20146 Hamburg, Germany.

H. A. J. Meijer, CIO, University of Groningen, 9722 JX Groningen, Netherlands. (e-mail: meijer@phys.rug.nl)

P. Monfray, Centre des Faibles Radioactivités, Bâtiment 709/ LMCE, 91191 Gif sur Yvette, France.

P. P. Tans, Climate Monitoring and Diagnostic Laboratory, NOAA, ERL 3, 325 Broadway, Boulder, CO 80303.

M. Trolier and J. W. C. White, Institute of Arctic and Alpine Research, University of Colorado, Campus Box 450, Boulder, CO 80303.

(Received November 18, 1995; revised June 25, 1996;
accepted July 12, 1996.)